Letter

Fluorogenic Detection of Monoamine Neurotransmitters in Live Cells

Kallol Bera, Anand Kant Das, Ananya Rakshit, Bidyut Sarkar, Anoop Rawat, Barun Kumar Maity, and Sudipta Maiti

ACS Chem. Neurosci., **Just Accepted Manuscript** • DOI: 10.1021/acschemneuro.7b00391 • Publication Date (Web): 11 Dec 2017

Fluorogenic Detection of Monoamine Neurotransmitters in Live Cells

Kallol Bera, Anand Kant Das, Ananya Rakshit, Bidyut Sarkar, Anoop Rawat, Barun Kumar Maity, Sudipta Maiti*

Department of Chemical Science, Tata Institute of Fundamental Research, Homi Bhabha Road, Colaba, Mumbai 400005, India

*e-mail: maiti@tifr.res.in

ABSTRACT:

Monoamine neurotransmission is key to neuromodulation, but imaging monoamines in live neurons has remained a challenge. Here we show that externally added ortho-phthalaldehyde (OPA) can permeate live cells and form bright fluorogenic adducts with intracellular monoamines (e.g. setrotonin, dopamine and nor-epinephrine) and with L-DOPA, which can be imaged sensitively using conventional single-photon excitation in a fluorescence microscope. The peak excitation and emission wavelengths (λ_{ex} = 401 nm and λ_{em} = 490 nm for serotonin; λ_{ex} = 446 nm and λ_{em} = 557 nm for dopamine; and λ_{ex} = 446 nm and λ_{em} = 544 nm for nor-epinephrine) are accessible to most modern confocal imaging instruments. The identity of monoamine containing structures (possibly neurotransmitter vesicles) in serotonergic RN46A cells is established by quasi-simultaneous imaging of serotonin using three-photon excitation microscopy. Mass spectrometry of cell extracts and of *in vitro* solutions helps us identify the chemical nature of the adducts, and establishes the reaction mechanisms. Our method has low toxicity, high selectivity and the ability to directly report the location and concentration of monoamines in live cells.

KEYWORDS: serotonin imaging, dopamine imaging, norepinephrine imaging, monoamine microscopy, Falck Hillarp method

Monoaminergic neurotransmission is important for processes related to mood, memory, reward and addiction, and in the context of diseases such as Parkinson's, Alzheimer's and depression [1-5]. Serotonin (5-HT), dopamine (DA) and norepinephrine (NE) are major monoamine neurotransmitters (MNT) in the brain, and the associated neuronal circuits are targets of many common pharmaceutical agents and drugs of abuse[6-8]. Monoamines are packed at a concentration of hundreds of mM in the neurotransmitter vesicles and to a level of tens of mM in some of the non-neuronal vesicles[9, 10]. Various strategies have been devised to detect and image these neurotransmitters in biological tissues with subcellular resolution. Microscopic imaging has been achieved with immunohistochemistry, but the cells have to be fixed[7]. Direct detection of 5-HT and DA with ultraviolet radiation has been attempted in live cells, but the UV radiation severely damages the cells, and available UV optics are of lower quality than visible wavelength optics[11, 12]. We and others have shown that three photon excitation can be effectively used to image serotonin in live neurons in the near-infra red by harnessing its intrinsic mid-ultraviolet autofluorescence[13-16]. Recently, we have also imaged intracellular DA with sub-μm three-dimensional resolution using two photon excitation[9], and demonstrated label-free ratiometric imaging of serotonin using three-photon excitation[17]. However, these techniques require a modified confocal microscope and pulsed femtosecond lasers. A detection method based on conventional (one-photon) excitation of fluorescence would be a boon to the community due to its accessibility and convenience.

Conventionally excited Fluorescent false neurotransmitters (FFNs) are selectively transported into vesicles containing monoamine transporters, and allow visualization of their exocytosis from individual presynaptic terminals[18-20]. However, FFNs are loaded into all secretory vesicles expressing VMAT (vesicular monoamine transporter) without discrimination to cell type, and therefore this approach cannot distinguish distinct cell populations that secrete a particular neurotransmitter[21]. Also, FFN fluorescence does not report the concentration of native neurotransmitters at any given location. In recent years, a number of cortical amine sensors have been reported, including fluorescent ribonucleopeptide (RNP) complexes[22], and boronic acid based fluorescent compounds[23, 24]. However, none of these methods represents a practical approach for *in vitro* and *in vivo* cellular analysis and imaging[25, 26]. It is thus imperative to explore a direct but benign method for their quantitative detection and visualization in live samples.

Since one-photon excitation (1-PE) in the visible cannot directly excite monoamines, we have to rely on the availability of fluorogenic reactants. Our method is inspired by the work of Falck and Hillarp, who discovered that exposing dry brain tissue to formaldehyde vapor (coupled with an oxidation step) imparts a bluish green fluorescence to monoaminergic cells[27, 28]. This enabled great progress in the field of monoaminergic neurotransmission, but the experimental requirements precluded the detection of monoamines in live cells[29].

Here, we have chosen a small organic molecule ortho-phthalaldehyde (OPA) to image and quantify native neurotransmitters in live neuronal cells[30-32]. We hypothesized that the highly nucleophilic primary amine group of MNT would readily form an isoindole with OPA, which will be further stabilized by the aromatic ring of the individual neurotransmitters, e.g. catechol amine (for DA) and indole (for 5-HT). The suggested reaction schemes are shown in Scheme 1. DA can give rise to compounds I, II and III, while 5-HT can yield IV, V and VI. The chemical reaction is related to that of formaldehyde in the Falck and Hillarp method, but we hypothesized that the extra phenyl ring would make the fluorescence more red-shifted, and might help the compound penetrate cell membranes better. The lower volatility of this compound, compared to that of formaldehyde, also makes it much easier and less toxic to handle[27, 28]. In addition, the extreme toxicity of formaldehyde does not permit its use in live cells, and this modification may make it less toxic to cells. We note that OPA has already been used for labeling histamine in plant tissue[33].

We tested our hypothesis *in vitro* by adding 500 µL of 100 µM aqueous MNT (DA or 5-HT) solution (colorless) to 500 µL of 100 µM aqueous OPA solution (colorless) separately. The solutions first turned violet and then changed to light green and ultimately to dark green, indicating the formation of MNT-OPA adduct. Mass spectrometry with a MALDI-TOF mass spectrometer revealed the formation of an isoindole ring [observed m/z for DA = 250.95, 368.33, 500.67, 619.94 (Fig. S1-7); m/z for 5-HT = 272.01, 274.35, 276.03, 293.11(Fig. S8-11)], and supported the proposed reaction scheme. For DA, we did not get the signature of the product III in the MALDI spectrum. However, we have found higher molecular mass which is possibly due to polymerization of DA-OPA adducts through catechol moiety. These polymerization reactions are described in the Fig. S3-S6. ESI-MS also supports the formation of adduct I (Fig. S7). For 5-HT, due to the absence of such reactive moiety, no polymerization was observed. ESI-MS further support the formation of product V and VI (Fig. S10, S11).

We then tested the fluorescence properties of the coloured products. The DA–OPA adduct has its excitation maximum (λ_{ex}) at 446 nm (Fig. 1A, magenta) and it emits in the region from 500-640 nm, with a peak at 557 nm (Fig. 1B, magenta). 5HT-OPA has the excitation maxima at 401 nm (Fig. 1A, red) and emits in the region of 470-620 nm, with a peak at 490 nm (Fig. 1B, red). Excitation and emission spectra of the OPA adducts of nor-epinephrine and L-DOPA are similar to that of DA-OPA (Fig. 1A and 1B, green and blue respectively). The reaction of MNT with OPA at pH 5.5 (estimated intravesicular pH) is nearly as efficient as in neutral pH 7.4 (Fig. 1C). OPA by itself has very little fluorescence (Fig. 1B, black), so the fluorescence enhancement for DA-OPA compared to OPA is > 20X (Fig. 2). A small peak at 532 nm is visible in the emission spectra. This is an artefact due to Raman scattering. We then tested the selectivity of this fluorogenic reaction against other common cellular components. The MNTs are derived from aromatic amino acids, so we investigated the selectivity of the sensor against the 20 common amino acids (listed in the legend of Fig. 2) at the same concentration. We also tested 17 other compounds using the same protocol (Fig. 2). The fluorescence intensity of no other compound exceeded 10% of the norepinephrine value. Epinephrine (EN) cannot form a fluorescence adduct

similar to norepinephrine due to its secondary amine functional group. We note that the intravesicular neurotransmitters concentration is >100 mM[14], so this level of enhancement by the other compounds would be expected to provide very low background fluorescence, resulting in very high selectivity for the neurotransmitters. The distinct emission spectra also provide some specificity amongst the well-detected compounds (5-HT, DA, NE and L-DOPA). Since intravesicular pH is ~ 5.5, we hypothesize that OPA can be used for intravesicular monoamine neurotransmitter detection in live cells.

Next, we attempted fluorogenic detection of 5-HT and DA in live cells, using the cell lines MN9D (dopaminergic neuronal cell line), RN46A (serotonergic neuronal cell line) and HEK293T (somatic cell line, used as a negative control). The cells were cultured according to protocols described elsewhere[9]. They were exposed to 100 μM OPA for 30 min at 37 °C, washed with Thomson's buffer to remove the remaining OPA, and imaged in a confocal microscope (Zeiss LSM710) using single photon excitation, with λ_{ex} = 488 nm. Fluorescence microscopic images showed that OPA penetrates cell membranes and reacts with MNT to form fluorescent products (Fig. 3). The enhancement of fluorescence was clear both for MN9D cells (compare Fig. 3a and 3c), and for RN46A cells (Fig. 3d and 3f). However, HEK293T cells show minimal increase of fluorescence (Fig. 3g and 3i). This is consistent with our expectation since HEK293T cells are not expected to contain monoaminergic vesicles. RN46A cells showed perinuclear luminescence in the cytoplasm, a pattern similar to that observed by us earlier using multiphoton microscopy[9, 29, 34]. However, MN9D cells showed a more diffuse cytoplasmic fluorescence in (Fig. 3c). This was also similar to the results obtained by us earlier using direct multiphoton imaging of dopamine[9]. To further verify whether the fluorescence indeed arises from the neurotransmitters, we probed a set of RN46A cells with direct three-photon excitation (3-PE) of serotonin at 740 nm (before OPA treatment, Fig. 3j), and subsequently by single photon excitation (1-PE) at 488 nm, after treating them with OPA (Fig. 3k). A Ti:Sapphire (MIRA, Coherent Inc., USA) laser operating at 740 nm and producing ~ 100 fs pulses (repetition rate, 76 MHz) was used for three photon excitation, and the cells were visualized using a custom-modified confocal microscope (LSM710, Zeiss, Germany). The radiation was separated from the serotonin fluorescence by a dichroic mirror (670dcxruv, Chroma, USA), and detected in the non-descanned part of the path.[17] The signal was passed through a 1-cm thick liquid $CuSO_4$ filter to block the excitation light. The filtered signal was detected by an analog photomultiplier tube (Model: P30A-01 Electron Tubes Limited, UK)[28, 29], which was externally connected to a custom signal input channel of the LSM 710 confocal microscope.

The images obtained from the 3-PE and 1-PE experiments showed very similar punctate objects, which may be vesicles or vesicular clusters. While there was some movement of these objects and the morphology of the cells did change somewhat in the intervening time, the similarities between the structures are obvious.

To further confirm that the same chemical reactions occurred inside the cells as had been observed *in vitro*, we performed mass spectroscopy of the cell extracts after OPA treatment.

RN46A cells were incubated with 100 μM OPA in Thomson's buffer for 30 min and then lysed by vigorous sonication. The lysate was collected for mass spectrometry. Though the small amounts obtained compromised the signal-to-noise ratio, the m/z peaks at 277.44 ($VI+H^+$), 297.51 ($IV+Na^+$), 313.0 ($IV+K^+$) and 331.82 ($V+K^+$) were observed in the OPA-treated cells (Fig. S12). The results are therefore consistent with the interpretation that the same products were formed inside the cell.

We further probed the applicability of our method by measuring the potential toxic effects of OPA in live cells. RN46A cells were plated on 96-well plates and were treated with various concentrations [10, 50, 100, 500, 1000 μM] of OPA for 24 hours. Cell viability was measured with MTT assay[35]. Cells were grown in 96-well plates and test compounds (10, 50, 100, 500, 1000 μM of OPA) were added to make a final volume of 100 μl/well and incubated according to the respective treatment time-points. 100 μl MTT solution (>98% purchased from SigmaAldrich) was added to each well to achieve a final concentrate ion of 0.5 mg/ml. The plate was incubated for 4 hours at 37°C. 100 μl of the solubilizing solution (50% (v/v) dimethylformamide (DMF) in 2% (v/v) glacial acetic acid, 20% (w/v) sodium dodecyl sulfate (SDS) was then added to each well to dissolve the formazan crystals. In order to ensure complete solubilization the plate was left in the 37°C incubator overnight. The absorbance was recorded at 570 nm on the following day. The results shown in Fig. 4 are the values of absorbance measurement (these values are not normalized), which provide a measure of the toxicity of the different concentrations of OPA. We found that OPA was not significantly toxic at 100 μM (which was the concentration used for the cell imaging studies) and only moderately toxic at 500 μM.

In conclusion, our results demonstrate that fluorogenic reactions with OPA can provide an accessible fluorescence imaging approach for monoamine neurotransmitters in live neuronal cells.

ASSOCIATED CONTENT

Reaction Scheme for Dopamine and OPA adduct formation, Mass Spectra of the Dopamine OPA adduct, MALDI spectra of the Dopamine-OPA adduct, Reaction mechanism for OPA dopamine adducts for product I and II, Plausible Reaction Mechanism for Higher Molecular Weight Adduct Formation, ESI-MS spectra of the Dopamin OPA adduct, OPA Serotonin Reaction, Mass spectra of the Serotonin OPA adduct, Fluorescence Spectroscopy of Dopamine-OPA and 5-HT:OPA adduct, MN9D, RN46A and HEK cell culture, confocal imaging studies of cells, Colocalization experiments (Multiphoton imaging followed by single photon), Mass Spectrometry with OPA treated RN46A cells.

AUTHOR INFORMATION

Corresponding Author

*Email: maiti@tifr.res.in

ORCID
Sudipta Maiti: 0000-0002-6540-7472

Present address: K.B., Division of Biology and Biological Engineering, California Institute of Technology, Pasadena, CA 91125
A.K.D., Vienna University of Technology, Institute for Applied Physics - Biophysics group, Getreidemarkt 9, 1060 Vienna, Austria
B.S., Molecular Spectroscopy Laboratory, RIKEN, 2-1, Hirosawa, Wako351-0198, Japan
A.R., University of Southern California, Los Angeles 90033, California

Notes

The authors declare no competing financial interest.

ACKNOWLEDGEMENTS

We thank Dr. Bappaditya Chandra (TIFR) and Prof. Soumen Basak (SINP) for their help and support.

REFERENCES

[1] Carlsson, A. (1987) Perspectives on the discovery of central monoaminergic neurotransmission, *Annu Rev Neurosci 10*, 19-40.
[2] Fuxe, K., Borroto-Escuela, D. O., Romero-Fernandez, W., Diaz-Cabiale, Z., Rivera, A., Ferraro, L., Tanganelli, S., Tarakanov, A. O., Garriga, P., Narvaez, J. A., Ciruela, F., Guescini, M., and Agnati, L. F. (2012) Extrasynaptic neurotransmission in the modulation of brain function. Focus on the striatal neuronal-glial networks, *Front Physiol 3*, 136.
[3] Das, A. K., Pandit, R., and Maiti, S. (2015) Effect of amyloids on the vesicular machinery: implications for somatic neurotransmission, *Philos Trans R Soc Lond B Biol Sci 370*.
[4] Ng, J., Papandreou, A., Heales, S. J., and Kurian, M. A. (2015) Monoamine neurotransmitter disorders--clinical advances and future perspectives, *Nat Rev Neurol 11*, 567-584.
[5] Kandel, E. R., and Mack, S. (2014) *Principles of neural science*.
[6] Chen, G., Yee, D. J., Gubernator, N. G., and Sames, D. (2005) Design of optical switches as metabolic indicators: new fluorogenic probes for monoamine oxidases (MAO A and B), *J Am Chem Soc 127*, 4544-4545.
[7] Shapiro, M. G., Westmeyer, G. G., Romero, P. A., Szablowski, J. O., Kuster, B., Shah, A., Otey, C. R., Langer, R., Arnold, F. H., and Jasanoff, A. (2010) Directed evolution of a

magnetic resonance imaging contrast agent for noninvasive imaging of dopamine, *Nat Biotechnol 28*, 264-270.

[8] Brustad, E. M., Lelyveld, V. S., Snow, C. D., Crook, N., Jung, S. T., Martinez, F. M., Scholl, T. J., Jasanoff, A., and Arnold, F. H. (2012) Structure-guided directed evolution of highly selective p450-based magnetic resonance imaging sensors for dopamine and serotonin, *J Mol Biol 422*, 245-262.

[9] Sarkar, B., Banerjee, A., Das, A. K., Nag, S., Kaushalya, S. K., Tripathy, U., Shameem, M., Shukla, S., and Maiti, S. (2014) Label-free dopamine imaging in live rat brain slices, *ACS Chem Neurosci 5*, 329-334.

[10] Hettie, K. S., Liu, X., Gillis, K. D., and Glass, T. E. (2013) Selective catecholamine recognition with NeuroSensor 521: a fluorescent sensor for the visualization of norepinephrine in fixed and live cells, *ACS Chem Neurosci 4*, 918-923.

[11] Rodriguez, P. C., Pereira, D. B., Borgkvist, A., Wong, M. Y., Barnard, C., Sonders, M. S., Zhang, H., Sames, D., and Sulzer, D. (2013) Fluorescent dopamine tracer resolves individual dopaminergic synapses and their activity in the brain, *Proc Natl Acad Sci U S A 110*, 870-875.

[12] Kruss, S., Landry, M. P., Vander Ende, E., Lima, B. M. A., Reuel, N. F., Zhang, J., Nelson, J., Mu, B., Hilmer, A., and Strano, M. (2014) Neurotransmitter Detection Using Corona Phase Molecular Recognition on Fluorescent Single-Walled Carbon Nanotube Sensors, *J Am Chem Soc 136*, 713-724.

[13] Balaji, J., Desai, R., and Maiti, S. (2004) Live cell ultraviolet microscopy: a comparison between two- and three-photon excitation, *Microsc Res Tech 63*, 67-71.

[14] Balaji, J., Desai, R., Kaushalya, S. K., Eaton, M. J., and Maiti, S. (2005) Quantitative measurement of serotonin synthesis and sequestration in individual live neuronal cells, *J Neurochem 95*, 1217-1226.

[15] Kaushalya, S. K., Desai, R., Arumugam, S., Ghosh, H., Balaji, J., and Maiti, S. (2008) Three-photon microscopy shows that somatic release can be a quantitatively significant component of serotonergic neurotransmission in the mammalian brain, *J Neurosci Res 86*, 3469-3480.

[16] Colgan, L. A., Putzier, I., and Levitan, E. S. (2009) Activity-dependent vesicular monoamine transporter-mediated depletion of the nucleus supports somatic release by serotonin neurons, *J Neurosci 29*, 15878-15887.

[17] Das, A. K., Maity, B. K., Surendran, D., Tripathy, U., and Maiti, S. (2017) Label-free Ratiometric Imaging of Serotonin in Live Cells, *ACS Chem Neurosci*.

[18] Lee, M., Gubernator, N. G., Sulzer, D., and Sames, D. (2010) Development of pH-responsive fluorescent false neurotransmitters, *J Am Chem Soc 132*, 8828-8830.

[19] Pereira, D. B., Schmitz, Y., Meszaros, J., Merchant, P., Hu, G., Li, S., Henke, A., Lizardi-Ortiz, J. E., Karpowicz, R. J., Jr., Morgenstern, T. J., Sonders, M. S., Kanter, E., Rodriguez, P. C., Mosharov, E. V., Sames, D., and Sulzer, D. (2016) Fluorescent false neurotransmitter reveals functionally silent dopamine vesicle clusters in the striatum, *Nat Neurosci 19*, 578-586.

[20] Gubernator, N. G., Zhang, H., Staal, R. G., Mosharov, E. V., Pereira, D. B., Yue, M., Balsanek, V., Vadola, P. A., Mukherjee, B., Edwards, R. H., Sulzer, D., and Sames, D. (2009) Fluorescent false neurotransmitters visualize dopamine release from individual presynaptic terminals, *Science 324*, 1441-1444.

[21] Sawamoto, K., Nakao, N., Kobayashi, K., Matsushita, N., Takahashi, H., Kakishita, K., Yamamoto, A., Yoshizaki, T., Terashima, T., Murakami, F., Itakura, T., and Okano, H. (2001) Visualization, direct isolation, and transplantation of midbrain dopaminergic neurons, *Proc Natl Acad Sci U S A 98*, 6423-6428.

[22] Liew, F. F., Hasegawa, T., Fukuda, M., Nakata, E., and Morii, T. (2011) Construction of dopamine sensors by using fluorescent ribonucleopeptide complexes, *Bioorg Med Chem 19*, 4473-4481.

[23] Secor, K. E., and Glass, T. E. (2004) Selective amine recognition: development of a chemosensor for dopamine and norepinephrine, *Org Lett 6*, 3727-3730.

[24] Guo, Z., Shin, I., and Yoon, J. (2012) Recognition and sensing of various species using boronic acid derivatives, *Chemical communications 48*, 5956-5967.

[25] Zhang, X., Zhu, Y., Li, X., Guo, X., Zhang, B., Jia, X., and Dai, B. (2016) A simple, fast and low-cost turn-on fluorescence method for dopamine detection using in situ reaction, *Analytica Chimica Acta 944*, 51-56.

[26] Zhang, X., Chen, X., Kai, S., Wang, H. Y., Yang, J., Wu, F. G., and Chen, Z. (2015) Highly sensitive and selective detection of dopamine using one-pot synthesized highly photoluminescent silicon nanoparticles, *Anal Chem 87*, 3360-3365.

[27] Falck, B., Hillarp, N. A., Thieme, G., and Torp, A. (1982) Fluorescence of catechol amines and related compounds condensed with formaldehyde, *Brain Res Bull 9*, xi-xv.

[28] Falck, B., and Torp, A. (1962) New evidence for the localization of noradrenalin in the adrenergic nerve terminals, *Med Exp Int J Exp Med 6*, 169-172.

[29] Kaushalya, S. K., Nag, S., Balaji, J., and Maiti, S. (2008) Serotonin: multiphoton imaging and relevant spectral data, pp 68601C-68601C-68608.

[30] Yu, C., Luo, M., Zeng, F., Zheng, F., and Wu, S. (2011) Mesoporous silica particles for selective detection of dopamine with beta-cyclodextrin as the selective barricade, *Chemical communications 47*, 9086-9088.

[31] Lin, V. S., Lai, C. Y., Huang, J., Song, S. A., and Xu, S. (2001) Molecular recognition inside of multifunctionalized mesoporous silicas: toward selective fluorescence detection of dopamine and glucosamine, *J Am Chem Soc 123*, 11510-11511.

[32] Radu, D. R., Lai, C. Y., Wiench, J. W., Pruski, M., and Lin, V. S. (2004) Gatekeeping layer effect: a poly(lactic acid)-coated mesoporous silica nanosphere-based fluorescence probe for detection of amino-containing neurotransmitters, *J Am Chem Soc 126*, 1640-1641.

[33] Roshchina, V. V. (2016) The Fluorescence Methods to Study Neurotransmitters (Biomediators) in Plant Cells, *J Fluoresc 26*, 1029-1043.

[34] Maiti, S., Shear, J. B., Williams, R. M., Zipfel, W. R., and Webb, W. W. (1997) Measuring serotonin distribution in live cells with three-photon excitation, *Science 275*, 530-532.

[35] Stockert, J. C., Blazquez-Castro, A., Canete, M., Horobin, R. W., and Villanueva, A. (2012) MTT assay for cell viability: Intracellular localization of the formazan product is in lipid droplets, *Acta Histochem 114*, 785-796.

FIGURE AND FIGURE CAPTIONS

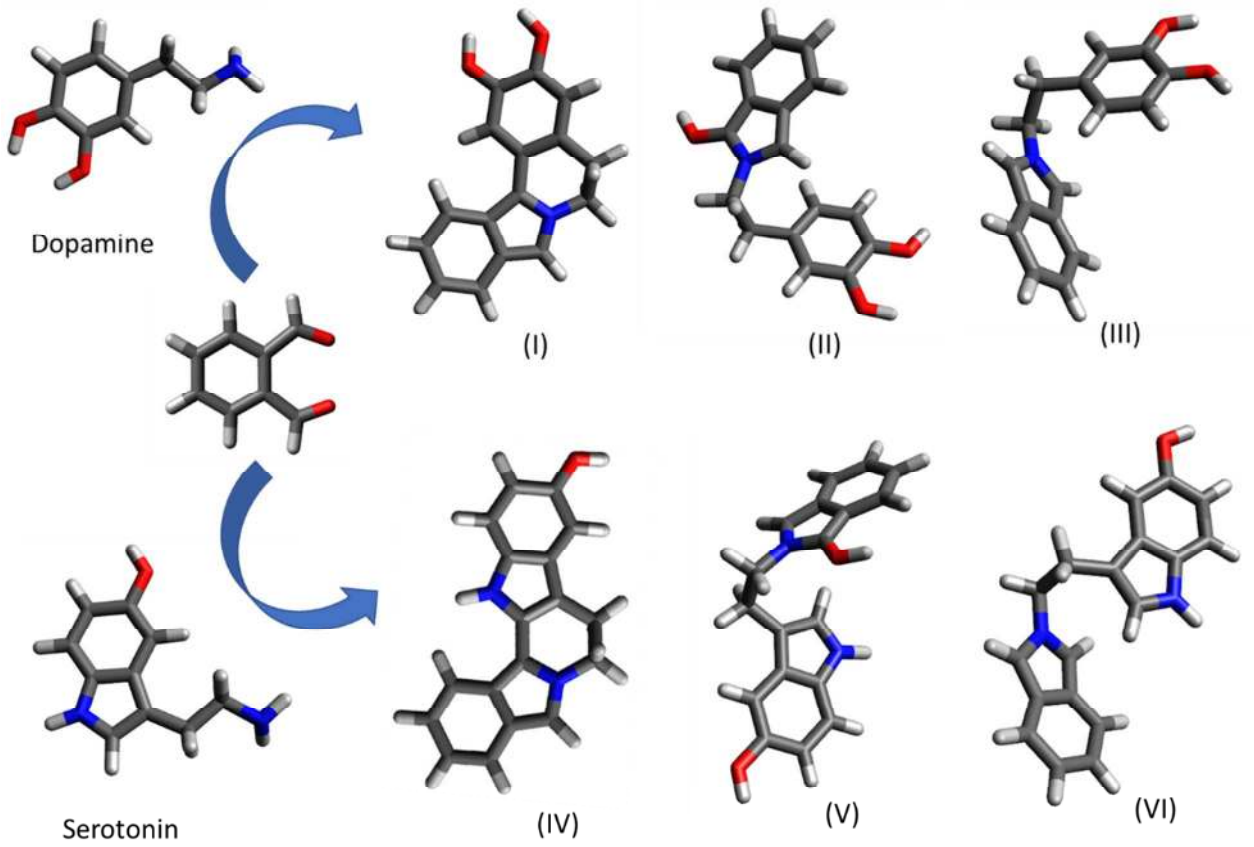

Scheme 1: Formation of possible products in a reaction between monoamine neurotransmitters (dopamine and serotonin) and OPA.

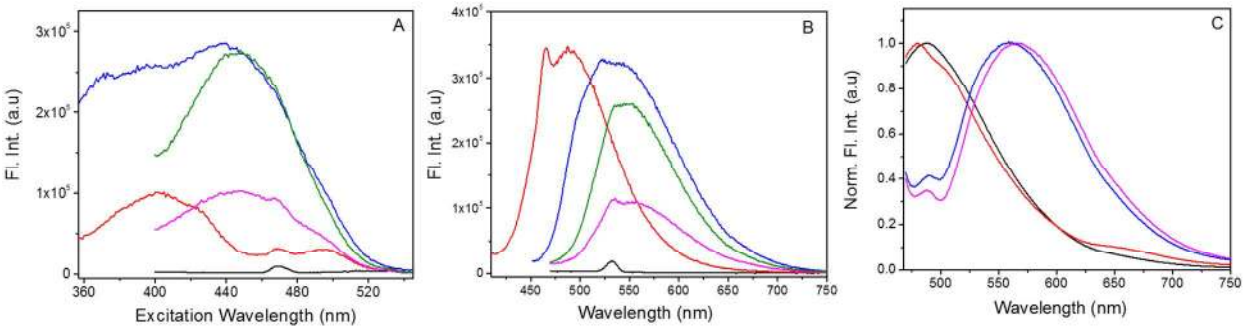

Figure 1: (A) and (B) represent excitation and emission spectra respectively of 10 μM OPA upon addition of 10 μM of each analyte in pH 7.4 PBS buffer. (OPA: Black, Serotonin + OPA: red, L-Dopa + OPA: blue, Dopamine + OPA: magenta, Nor-epinephrine + OPA: green). For recording excitation spectra emission was monitored at 560 nm. For the emission spectra, the excitation wavelengths for OPA, serotonin, L-dopa, dopamine and nor-epinephrine are at 450 nm, 400 nm, 440 nm, 450 nm and 450 nm respectively. In (C), black and red traces represent normalized emission spectra of 100 μM serotonin + 100 μM OPA at pH 7.4 and 5.5 respectively, while blue and magenta represent100 μM dopamine + 100 μM OPA at pH 7.4 and 5.5 respectively.

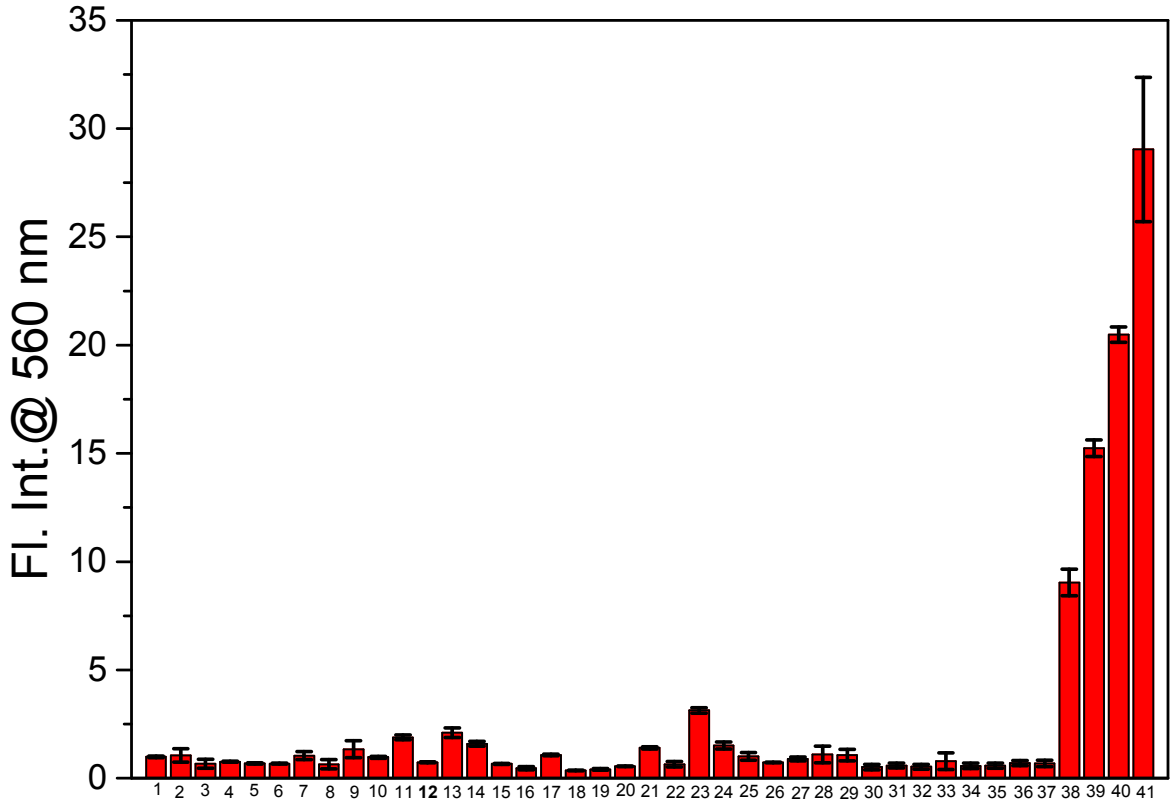

Figure 2: Fluorescence intensity (λ_{ex} = 450 nm, λ_{em} = 560 nm, unless mentioned otherwise) of 10 μM OPA upon addition of 10 μM of each analyte in pH 7.4 PBS buffer (λ_{ex} = 450 nm). 1: Ascorbic acid; 2: Adenosine monophosphate; 3: Arginine; 4: BSA; 5: Citric acid ; 6: Cysteine; 7: Glucose; 8: Glutamic acid; 9: Glycine; 10: Guanidine; 11: Guanosine; 12: Homo-cysteine thiolactone; 13: Histidine; 14: HSA; 15: Imidazole; 16: Isoleucine; 17: Lipoic acid; 18: Lysine; 19: Cysteine + Lysine; 20: Methionine; 21: NADPH; 22: Phenylalanine; 23: Piperonyleamine; 24: Serine; 25: Thiamine; 26: Thymine; 27: Tryptophanamide; 28: Tryptophan; 29: Tyrosine; 30: OPA; 31: PCA; 32: Epinephrine; 33: Glutamine; 34: Na^{+}; 35: Mg^{2+}; 36: K^{+}; 37: Ca^{2+}; 38: Serotonin (λ_{em} = 490 nm); 39: L-Dopa; 40: Dopamine; 41: Nor-epinephrine.

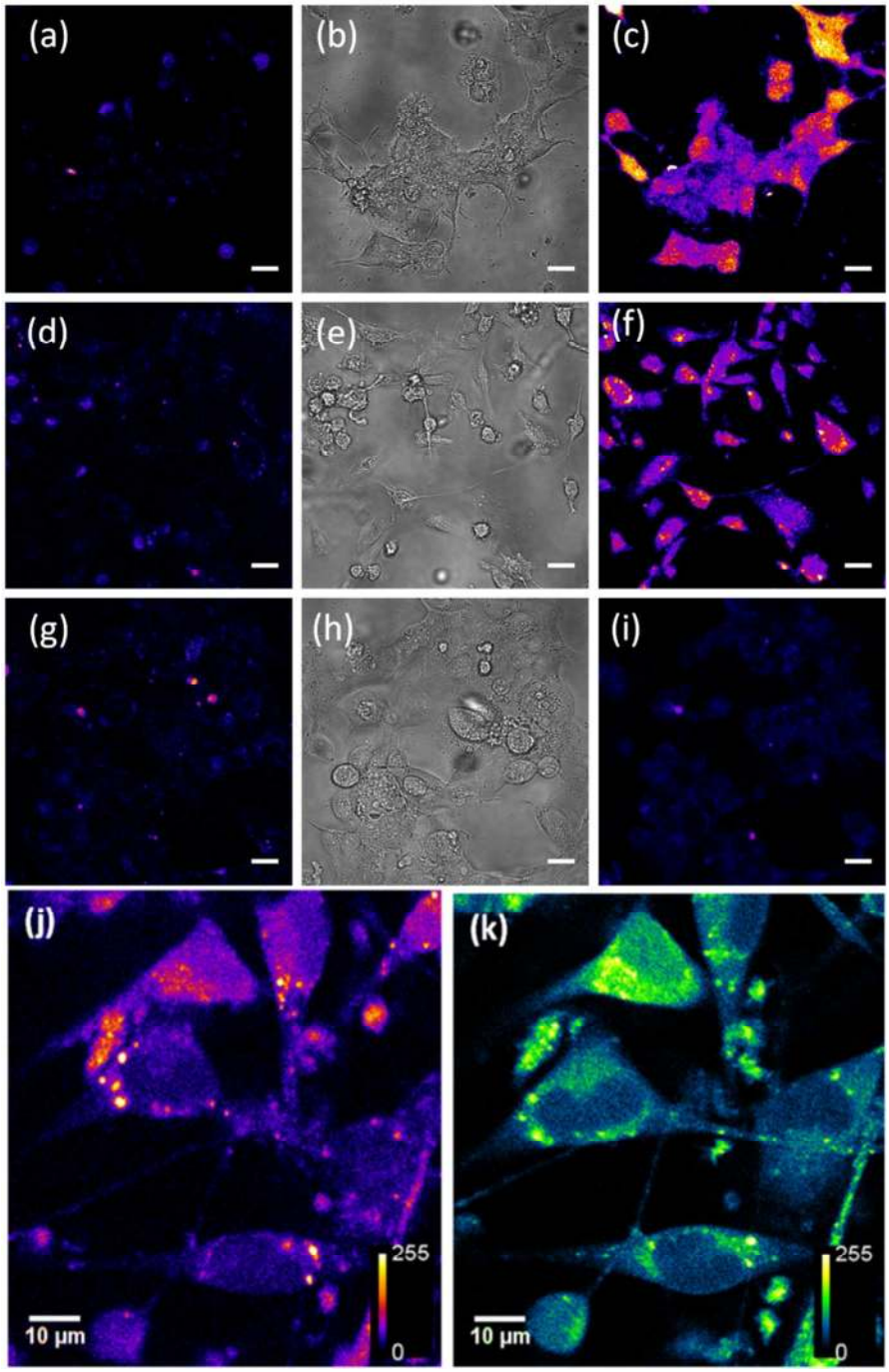

Figure 3: (a – c) : MN9D cells incubated with 100 µM OPA (a) 0 min after incubation, (b) transmission image, (c) 30 min after incubation. (d-f) RN46A incubated with 100 µM OPA (d) 0 min after incubation, (e) transmission image, (f) 30 min after incubation. (g-i) HEK (Control) cells incubated with 100 µM OPA. (g) 0 min after incubation, (h) transmission image, (i) 30 min after incubation. (j – k) Comparison of observed serotonin containing structures in RN46A cells. (j) multiphoton image (λ_{ex} = 740 nm) (k) single photon confocal image (λ_{ex} = 488 nm), after 100 µM OPA treatment. Scale bar is 20 µm (for a-i), 10 µm (for j-k).

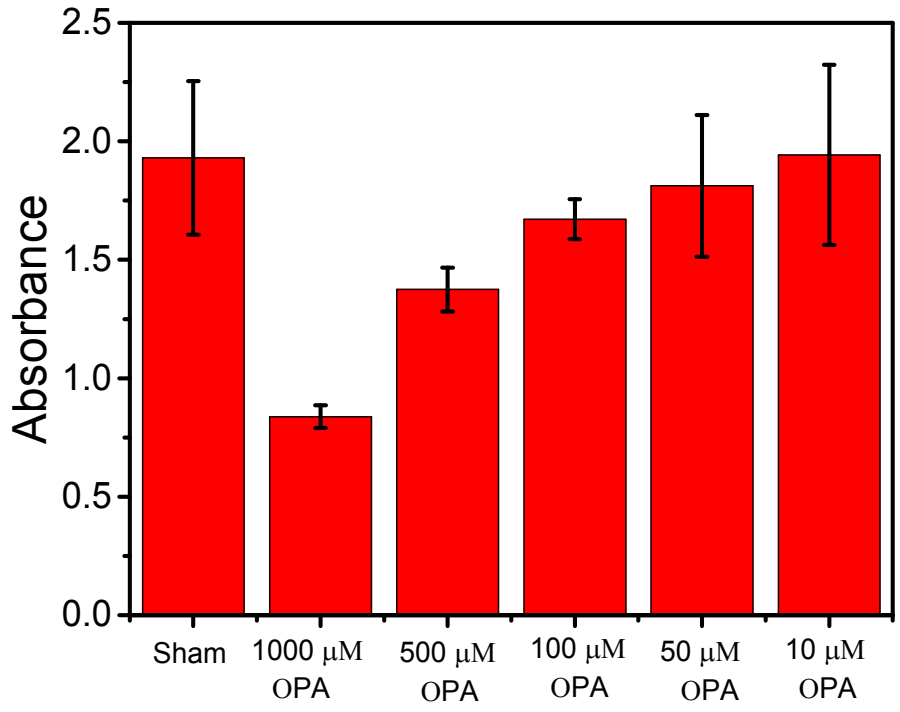

Figure 4: Toxicity of different concentrations of OPA measured for RN46A cells using MTT assay.

Table of Content

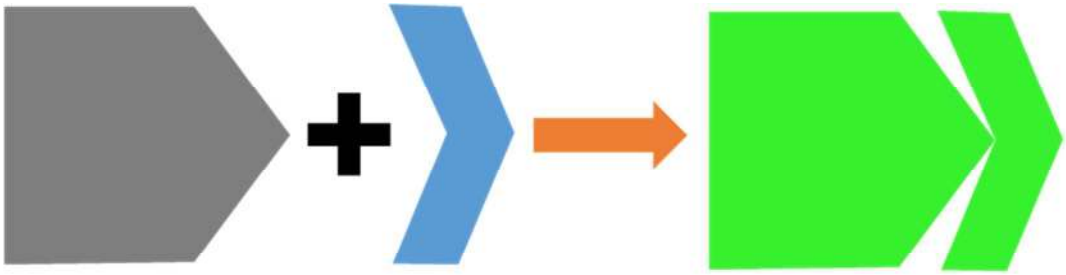

Neurotransmitter Probe Fluorescent Adduct